RSC Publishing RSC Advances

Novel synthesis of core-shell urchin-like ZnO coated carbonyl iron microparticles with enhanced magnetorheological activity

Journal:	*RSC Advances*
Manuscript ID:	RA-ART-09-2013-044982
Article Type:	Paper
Date Submitted by the Author:	10-Sep-2013

Complete List of Authors:	Machovsky, Michal; Centre of Polymer Systems Tomas Bata University in Zlin, University Institute; Polymer Centre, Tomas Bata University in Zlin, Faculty of Technology Mrlík, Miroslav; Tomas Bata University in Zlin, Centre of Polymer Systems; Tomas Bata University in Zlin, Polymer Centre Kuritka, Ivo; Centre of Polymer Systems Tomas Bata University in Zlin, University Institute; Polymer Centre, Tomas Bata University in Zlin, Faculty of Technology Pavlinek, Vladimir; Centre of Polymer Systems Tomas Bata University in Zlin, University Institute; Polymer Centre, Tomas Bata University in Zlin, Faculty of Technology Babayan, Vladimir; Centre of Polymer Systems Tomas Bata University in Zlin, University Institute; Polymer Centre, Tomas Bata University in Zlin, Faculty of Technology

RSC Advances

An international journal to further the chemical sciences

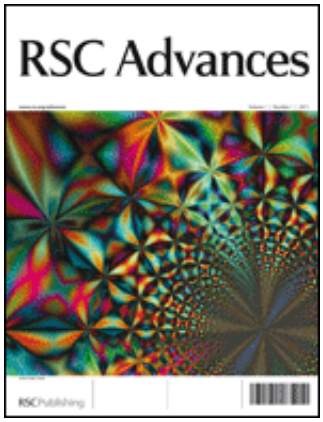

RSC Advances is an international, peer-reviewed, online journal covering all of the chemical sciences, including interdisciplinary fields.

The **criteria for publication** are that the experimental and/ or theoretical **work must be high quality, well conducted adding to the development of the field**.

Thank you for your assistance in evaluating this manuscript.

Guidelines to the referees

Referees have the responsibility to treat the manuscript as confidential. Please be aware of our **Ethical Guidelines**, which contain full information on the responsibilities of referees and authors, and our **Refereeing Procedure and Policy**.

It is essential that all research work reported in *RSC Advances* is well-carried out and well-characterised. There should be enough supporting evidence for the claims made in the manuscript.

When preparing your report, please:
- comment on the originality and scientific reliability of the work
- state clearly whether you would like to see the article accepted or rejected and give detailed comments (with references, as appropriate) that will both help the Editor to make a decision on the article and the authors to improve it

Please inform the Editor if:
- there is a conflict of interest
- there is a significant part of the work which you are not able to referee with confidence
- the work, or a significant part of the work, has previously been published
- you believe the work, or a significant part of the work, is currently submitted elsewhere
- the work represents part of an unduly fragmented investigation

For further information about *RSC Advances*, please visit: www.rsc.org/advances or contact us by email: advances@rsc.org.

Centre of Polymer Systems
University Institute
Tomas Bata University in Zlin
Nad Ovcirnou 3685
760 01 Zlin
Czech Republic

10th September 2013

Prof. James D Batteas
Texas A&M University,
USA

Dear Prof. James D Batteas

Enclosed please find the manuscript entitled "**Novel synthesis of core-shell urchin-like ZnO coated carbonyl iron microparticles with enhanced magnetorheological activity**". The paper is intended for publication in *RSC advances* if you consider it suitable. We believe that this article describing novel synthesis of inorganic-inorganic core-shell particles with unique urchin-like morphology having extraordinary rheological properties under applied magnetic field and further, exhibiting considerably enhanced sedimentation and thermo-oxidation stability with great potential in wide areas of industrial applications. We also hope that article is matching with the scope of your journal categories "*Inorganic*" and "*Rheology and colloids*" and is attractive enough in the same time.

Sincerely yours

Miroslav Mrlík *et al.*
(Corresponding author)

E-mail: mrlik@ft.utb.cz
tel: +420 57 603 8128, fax: +420 576 031 444

Synthesis of core-shell urchin-like ZnO coated carbonyl iron microparticles and their magnetorheological activity

Michal Machovsky[1,2], Miroslav Mrlik[1,2*],Ivo Kuritka[1,2], Vladimir Pavlinek[1,2], Vladimir Babayan[1,2]

[1] *Centre of Polymer Systems, University Institute, Tomas Bata University in Zlin, Nad Ovcirnou 3685, 760 01 Zlin, Czech Republic*
[2] *Polymer Centre, Faculty of Technology, Tomas Bata University in Zlin, TGM 275, 762 72 Zlin, Czech Republic*
*mrlik@ft.utb.cz
tel: +420 57 603 8128
fax: +420 57 603 1444

ABSTRACT

The overall stability (thermo-oxidation, sedimentation) of the MR suspensions is a crucial problem decreasing their potential applicability in the real life. In this study the unique functional coating of carbonyl iron (CI) particles with ZnO structures was presented in order to develop new MR suspension based on the core-shell ZnO/CI urchin-like dispersed particles. The two-step synthesis provides the suitable core-shell particles with improved sedimentation and also thermo-oxidation stability. Moreover, due to the enhanced sedimentation stability core-shell based suspensions exhibit higher values of the yield stress than those of bare CI based suspensions at 20 wt. % particle concentration. The suspension with 60 wt. % particle concentration reaches value of the yield stress around 2.2 kPa at 272 mT. The excellent MR efficiency of the core-shell ZnO/CI based suspension at elevated temperatures was observed. Finally, the dimorphic particle based suspension was prepared when ratio between the carbonyl iron and core-shell urchin-like particles was 1:1. The highest yield stress was obtained in the case of dimorphic particles-based suspension due to good magnetic properties of bare carbonyl iron and mechanical gripping between core-shell ZnO/CI urchin-like particles.

KEYWORDS: Core-shell, inorganic-inorganic, urchin-like, ZnO, carbonyl iron, magnetorheology, thermal stability, sedimentation stability.

1. Introduction

Magnetorheological fluids (MRF) represent a class of smart matters consisting of magnetic particles and liquid medium, whose rheological characteristics show fast and reversible transition from a liquid-like to solid-like state when they are exposed to external magnetic fields [1-5]. In the absence of a magnetic field, the particles are randomly dispersed in the carrier liquid and MR fluid exhibits Newtonian-like behaviour. After applying magnetic field, the dispersed particles are magnetized and the interaction between the induced dipoles cause the particles form internal field-induced structures, parallel to the applied field [6-11]. Development of such structures is resulting in the increase of the suspension viscosity and transition from Newtonian to pseudoplastic behaviour appears with certain level of the yield stress [12-15].

There is a wide range of technological applications that benefit from materials able to provide rapid-response interfaces between electronic controls and mechanical systems, including rotary brakes, dampers, shock absorbers, torque transducers, etc. [16-19]. Besides established commercial use of MR fluids in automotive industry, developments might be expected in field of civil and aerospace engineering especially [20, 21]. Moreover, presently the new medical applications of MR fluids in the cancer treatment by hyperthermia method started to be developed [22].

In spite of the essential advantages of such materials, there are still two main limitations inhibiting of their impulsive expansion to the common real-life applications. The first one is the poor stability against sedimentation, due to the considerable difference between solid particles and liquid medium densities. There are several options how to improve such behaviour i.e. using thixotropic agents, surfactants [23] or utilizing bidispersed or dimorphic particle mixtures [24, 25]. Also employing of the core-shell particles based on inorganic-polymer [26-33] or inorganic-MWCNT [34-36] as well as inorganic-inorganic coatings enhance the mentioned sedimentation stability. The second disadvantage is insufficient thermal stability of the iron particles, whose oxidation after they are exposed to the elevated temperature considerably decreases the magnetorheological properties [37]. Thus, the modification of the particles especially, using various polymers [38-40] is usually applied.

In our preceding study [41] the coating of the carbonyl iron particles with low molecular weight substance cholesteryl chloroformate was performed. Such coating provided particles

with slightly enhanced thermooxidation stability and moderately increased sedimentation stability of their silicone oil suspension.

Therefore, this study is concentrated on the preparation of the core-shell inorganic-inorganic ZnO urchin-like coated carbonyl iron microparticles via two-step synthesis. The successful synthesis was confirmed by scanning electron microscopy (SEM), energy dispersive X-ray spectroscopy (EDX) and X-ray diffraction spectroscopy (XRD) techniques. Rheological properties in the presence as well as in the absence of the external magnetic field of both bare carbonyl iron and the urchin-like ZnO/CI core-shell particles-based suspensions were investigated. Finally, the crucial parameters such as thermooxidation and long-term sedimentation stability were also evaluated

2. Materials and Methods

2.1 Materials

Carbonyl iron microparticles (SL grade, α -iron content >99.5 %, BASF, Germany), zinc acetate dihydrate $Zn(CH_3COO)_2.2H_2O$ (ZAD), zinc nitrate hexahydrate $Zn(NO_3)_2.6H_2O$ and hexamethylenetetramine $(CH_2)_6N_4$ (HMTA) were all purchased from PENTA (Czech Republic) and used as received without further purification. Demineralized water with conductivity about 10^{-7} Scm^{-1} and ethanol were used throughout experiments.

2.2 Synthesis of core-shell urchin-like ZnO/CI particles

ZnO/CI composite particles were prepared in two steps. The first step involved "seeding" of CI particles with ZnO nanocrystals via modified procedure proposed originally by Spanhel [42]. Briefly, 0.005 M solution obtained by dissolving 0.165 g of ZAD in 150 ml of ethanol was added to the flask with 1 g of CI particles and sonicated for 2 minutes. After that, the flask was placed on the hot plate and heated at 80 °C. The dispersion was agitated mechanically by stirrer speed set at 900 rpm for 2 h before being left to cool down to the room temperature naturally. Than, the dispersion was washed several times with ethanol, filtered, and collected particles were dried at 60 °C.

After seeding procedure, CI_{seed} particles coated with ZnO nanocrystals were used as a substrate for the hydrothermal growth of ZnO nanorods. The growth was carried out in the mixture of aqueous solution of zinc nitrate hexahydrate (0.05 M) and HMTA (0.05 M) at 80 °C under mechanical stirring with agitator speed set up 650 rpm for 2 h. After cooling, the

particles were washed thoroughly with distilled water, filtered and dried at 60 °C. Prepared CI/ZnO particles were characterized and used as a dispersed phase for magnetorheological suspensions.

2.3 Particles characterization

Crystalline phase of particles was characterized by the powder X-ray diffractometer X´Pert PRO X-ray (PANalytical, The Netherlands) with a Cu-K_α X-ray source (λ = 1.5418 Å) in the diffraction angle range 5-85° 2θ. The morphology was examined by scanning electron microscope Vega II/LMU (Tescan, Czech Republic) equipped with EDX-System OXFORD INCA Energy 200 (OXFORD INSTRUMENTS, UK)
The magnetic properties were studied using a vibrating sample magnetometer VSM 7400 (Lake Shore, United States). Thermogravimetric analysis (TGA) was carried out by the thermogravimeter Q500 (TA instruments, United States) in the temperature range from 25 to 800°C at a heating rate 20°C min^{-1} in flowing air (30 sccm).

2.4 Suspension preparation and rheological measurements

ZnO/CI core-shell particles were suspended in silicone oil (Lukosiol M 200, viscosity η_c = 194 mPa s, density d_c = 0.970 g cm^{-3}, relative permittivity ε' = 2.89, loss factor tan δ = 0.0001, Chemical Works Kolín, Czech Republic) with 20, 40, and 60 wt. % particle concentrations. The suspensions were mechanically stirred before each measurement. The rheological properties under an external magnetic fields in the range 0–300 mT were investigated using a rotational rheometer Physica MCR502 (Anton Paar GmbH, Austria) equipped with a Physica MRD 170/1T magneto-cell. The true magnetic flux density was measured using a Hall probe. Rheological measurements were performed at temperature 25, 45, 65, 85 and 105 °C.

2.5 Particle sedimentation

The silicone oil suspensions containing 40 wt. % of both bare CI and ZnO/CI urchin-like particles were firstly mechanically stirred and then placed to the vials and sedimentation test was performed. The sedimentation ratio, as a ratio between the height of the suspension in the

vial at the beginning of test and the height of the particle rich phase after certain time period, was evaluated as a measure of sedimentation stability within the 30 hours.

3. Results and Discussion

3.1. XRD characterization

Powder XRD patterns of bare CI, CI seed, and CI/ZnO composites are shown in Figure 1. For CI particles, peaks observed at 2θ = 44.6°, 65°, and 82.3° (marked by diamonds) correspond to (110), (200), and (211) reflections of iron with the cubic structure (ICDD PDF-2 entry 01-087-0722). The diffraction patterns of seeded CI sample seem to remain unchanged comparing to diffractogram of bare CI and no peaks corresponding to ZnO crystal phase were detected. On the other hand the presence of seeds on the CI particle surface was further confirmed by both SEM as well as by EDX. Diffraction patterns of CI/ZnO composite contain peaks related to iron cubic structure peaks at 2θ = 44.6°, 65°, and 82.3° and as expected also peaks located at 2θ = 31.7°, 34.3°, 36.1°, 47.4°, 56.5°, 62.8°, 67.8° and 68.9° (marked by stars) which correspond well to hexagonal wurtzite crystal structure of ZnO (ICDD PDF-2 entry 01-079-0207).

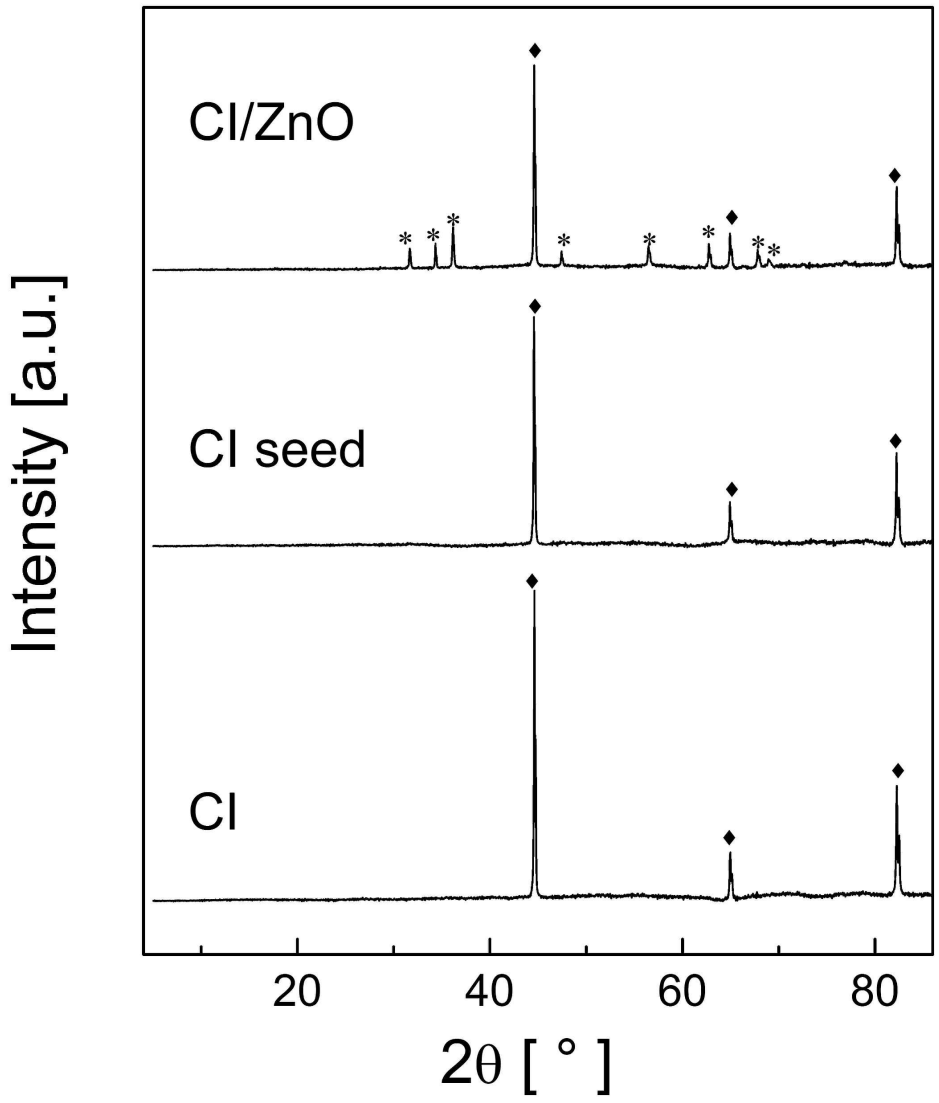

Figure 1: XRD patterns of particles, where peaks representing CI are marked as (diamonds) and peaks representing ZnO are marked as (stars).

3.2. SEM analysis

Scanning electron micrographs of bare CI powder are shown in Figure 2(a,b). It can be seen that particles are of the spherical shape with some bigger particles about 9 μm in diameter, but the most of them being in the range of 1–4 μm. Figure 2(c,d) shows morphology of CI particles after seeding (seeded CI) in ZAD ethanol solution. Nanoparticles with the size of about 150 nm are clearly seen in the enlarged image (Figure 2d) although no ZnO diffraction pattern was detected by XRD measurement. Therefore, energy dispersive X-ray (EDX)

elemental microanalysis was performed to confirm the presence of zinc and oxygen. Zinc as well as carbon traces in the material were clearly revealed besides the strong signal of iron dominating the whole spectrum in Figure 3. However, oxygen's Kα emission can be only found hidden in the low energy shoulder of the broad iron's L series emission peak. Precise quantification of zinc and oxygen mass ratio cannot be made due to the aforementioned poor spectral line resolution and because of the generally low sensitivity and semi-quantitativeness of the used EDX technique. The product of hydrothermal growth of ZnO on seeded CI particles is shown in Figure 2(e,f). Finally ZnO microrods are growing radially onto CI particles surface forming urchin-like structure of ZnO decorated spherical CI particles. The ZnO microrods are about 100–200 nm in diameter and 1–1.5 μm in length. It should be noted that the diameter of microrods is approximately the same as dimensions of seeded ZnO nanocrystals. However, the microrods are crowded closely together much more than it can be expected according to the surface coverage density of nanoseeds observed in Fig. 2(c,d). It seems that the seeded particles are multifaceted centers of branched growth of single rods.

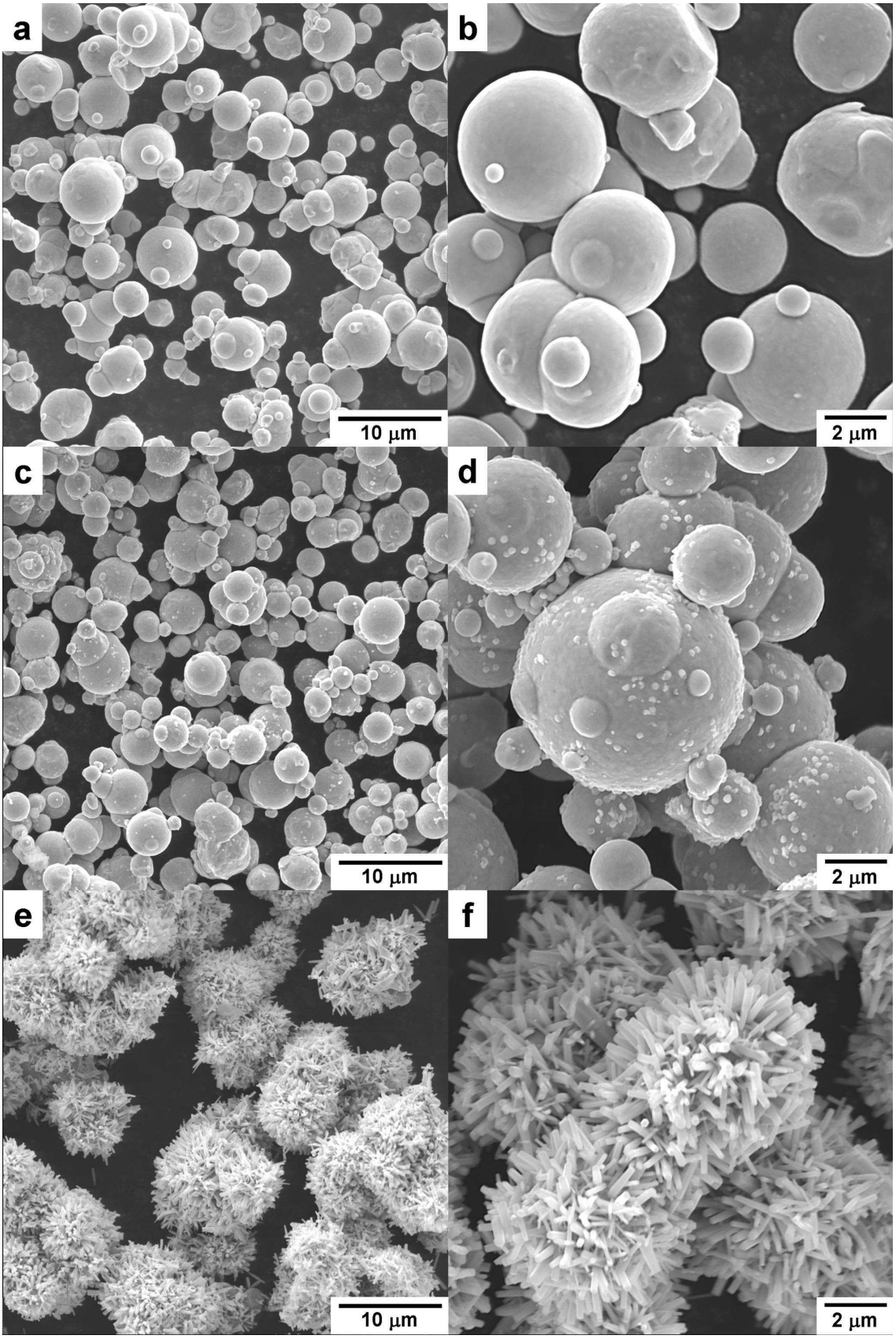
a
10 μm
b
2 μm
c
10 μm
d
2 μm
e
10 μm
f
2 μm

Figure 2: SEM micrographs of bare CI (a, b), ZnO seeded CI (c, d), ZnO/CI urchin-like (e, f) particles at various magnifications.

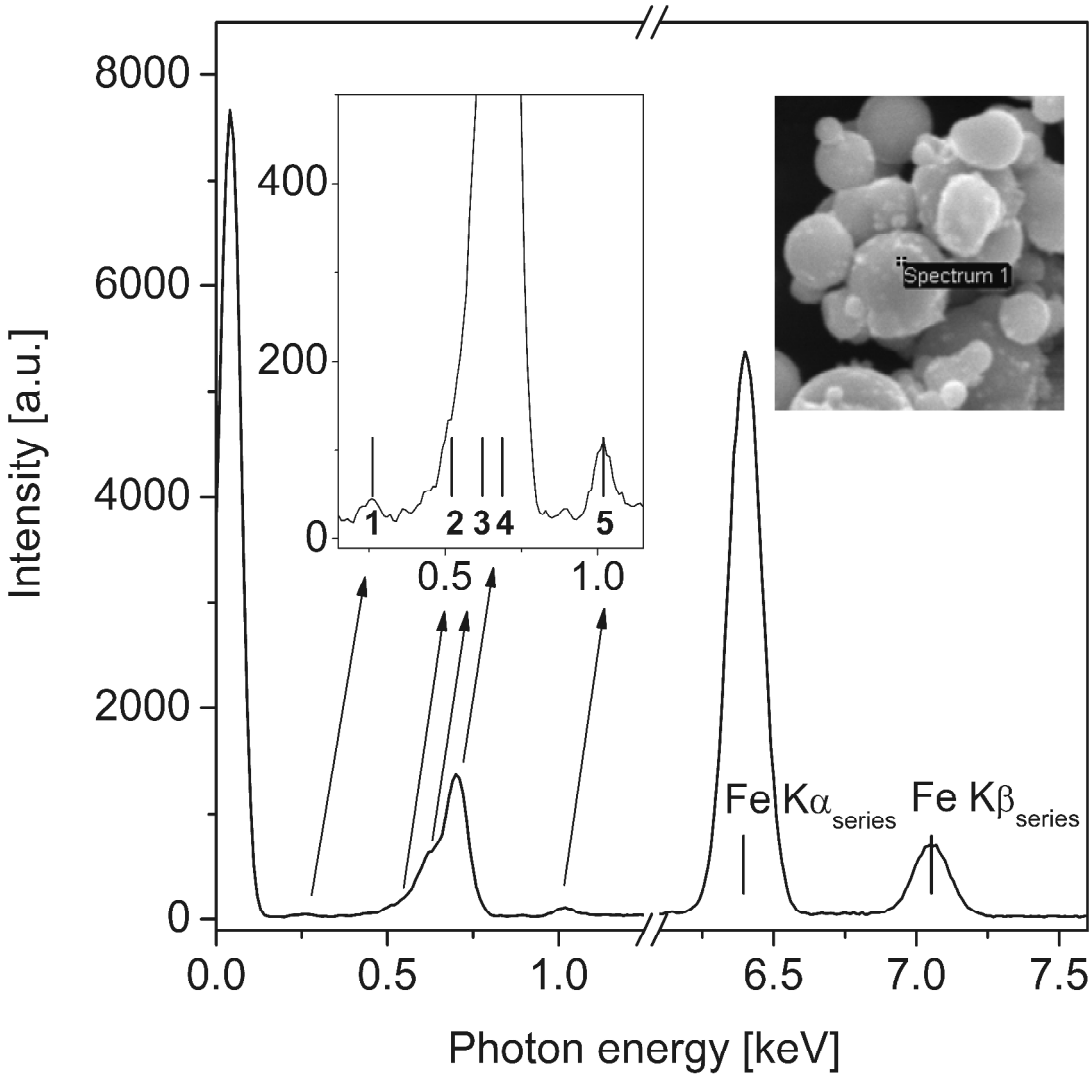

Figure 3: EDX spectrum of a surface spot on seeded CI particle, magnified details in inset graph: 1 – C Kα line, 2 – O K Kα line, 3 and 4 – Fe L lines, 5 – Zn L lines, the inset image shows the spot on the CI particle, where the point spectrum was collected from.

3.3 Magnetic properties

Magnetostatic properties were measured by vibrating sample magnetometry and the resulting hysteresis loops of bare CI, ZnO seeded CI and CI/ZnO particles are shown in Figure 4. All samples exhibit a soft magnetic behavior with negligible remanence and coercivity. Whereas the values of remanence and coercivity remained almost unchanged, the saturation magnetization (M_s) decreased significantly from 182.6 emu g^{-1} for bare CI to 129 emu g^{-1} for CI/ZnO particles. The decrease in saturation magnetization can be reasonably attributed to diluting contribution of non-magnetic ZnO in sampling volume. However, the saturation magnetization value of ZN seeded CI sample (159.5 emu g^{-1}) is significantly lower than that of bare CI (182.6 emu g^{-1}) although the ZnO fraction is negligible. Another mechanism than dilution but related with the surface thin semiconducting film must be active in such phenomena. Magnetic domain wall pinning can be employed for its explanation similarly as it was already demonstrated being crucial for polyaniline thin film covered core-shell CI particles.

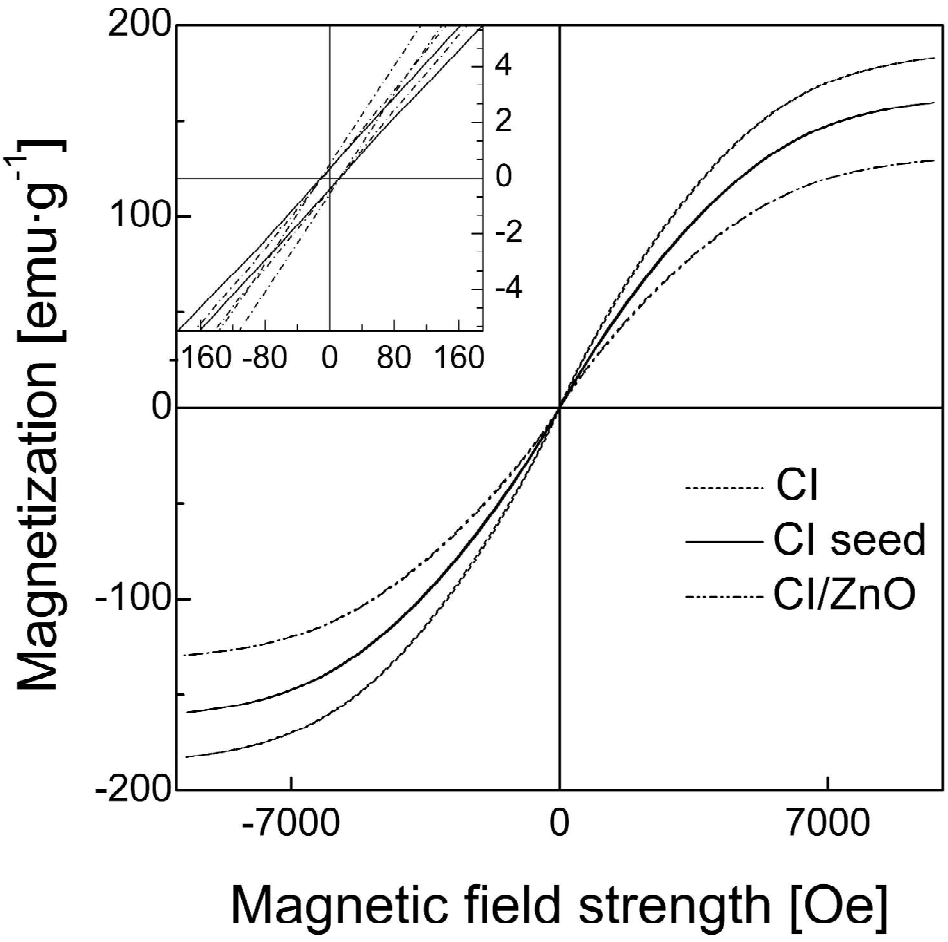

Figure 4: VSM spectra of the bare CI (dashed line), ZnO seeded CI (solid line) and ZnO/CI urchin-like (dash dot line) particles.

3.4 Thermo-oxidation and sedimentation stability

Thermogravimetric analysis under dynamic air atmosphere is an indicative experiment of thermo-oxidative stability. Obtained results are shown in Figure 5. The dense surface coverage of reactive and easily corrodible CI particles by semiconducting microrods enhanced the stability of CI towards oxidation even at elevated temperatures. First, the total mass increase due to oxidation was lower for CI/ZnO than for bare CI particles over the same temperature range. In next, the onset temperature as well as the maximum rate of oxidation is

shifted of more than about 200°C towards higher temperature for CI/ZnO which can be considered as a significant effect.

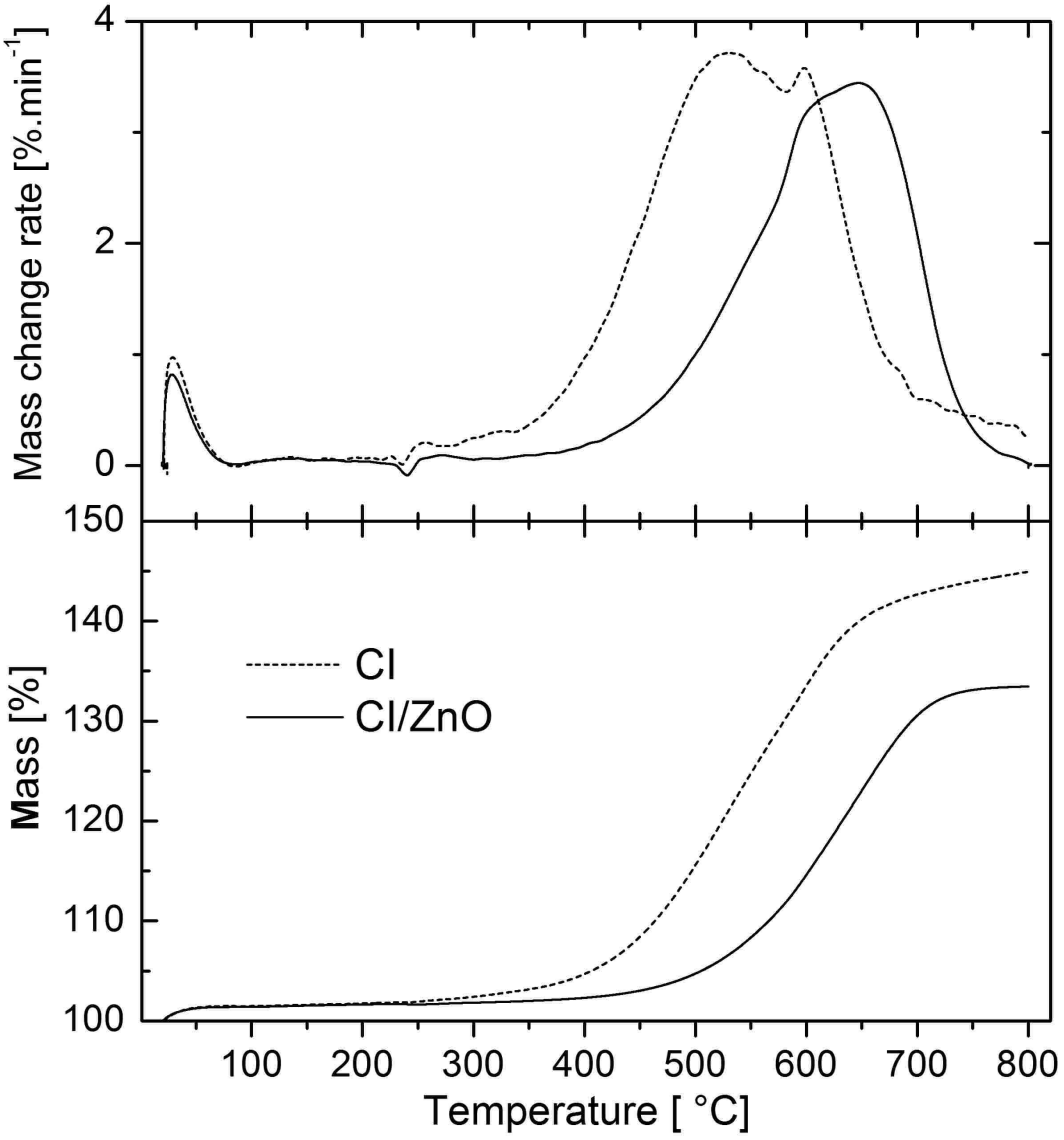

Figure 5: TGA curves and their derivatives of bare CI (dash dot line) and ZnO/CI urchine-like (solid line) particles.

Sedimentation stability is very important factor influencing the magnetorheological (MR) activity of the suspensions. Systems with poor long-term behaviour also exhibit reduced MR efficiency, due to fast particle settling. Such systems are not able to further create internal

structures of suitable toughness after application of the external field and their application in real-life application is therefore limited. Thus the sedimentation ratio as a parameter representing the stability of the suspension in the time was investigated. As can be seen in the Figure 6 the sedimentation ratio of suspension containing bare CI particles is nearly on 40 % of the maxima after 5 hours while ZnO/CI urchin-like are on the 60 %. Furthermore, within the another 25 hours of the test suspensions exhibit nearly same behaviour and the values of the sedimentation ration was fixed on the 30 % for bare CI-based suspension and 50 % for ZnO/CI urchin-like based suspensions, probably due to the partial decreased density of the core-shell particles and also because of the extraordinary urchin-like shape contributing to the enhanced sedimentation stability.

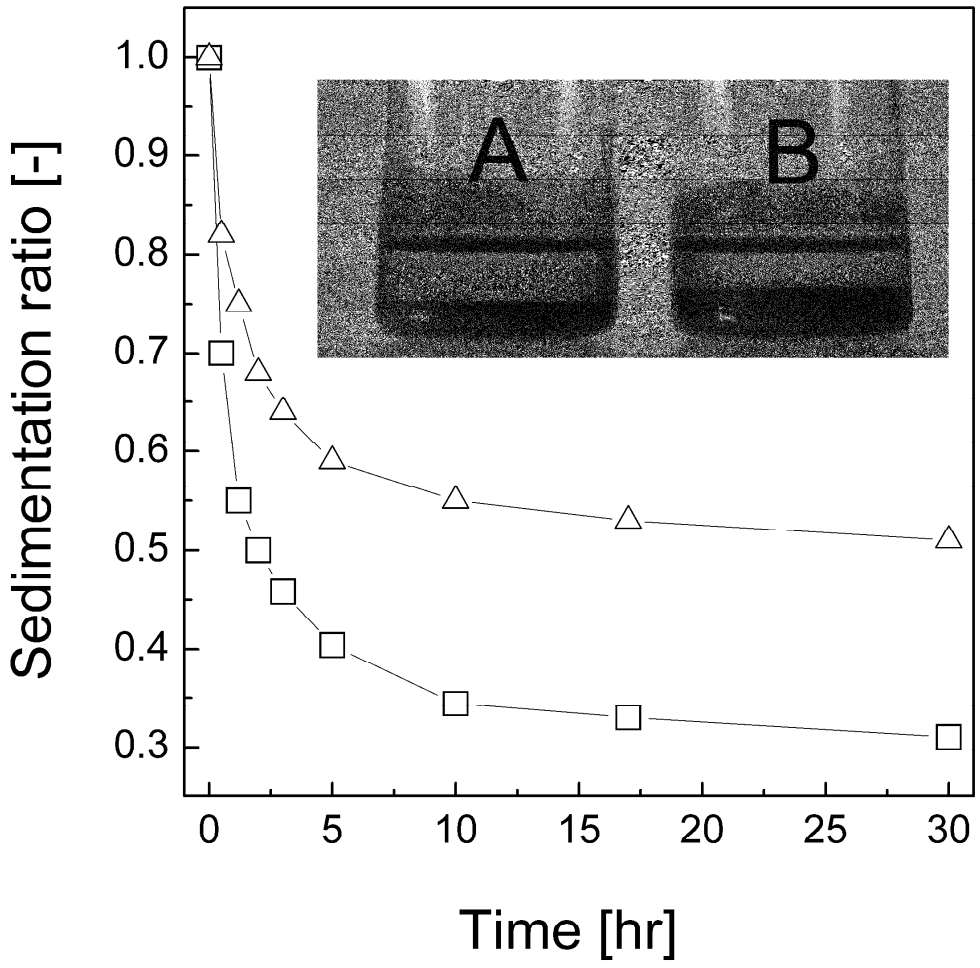

Figure 6: Sedimentation stability of the bare CI particle suspension measuring jug A (□) and ZnO/CI urchin-like particle suspension measuring jug B (△).

3.5 Magnetorheological behaviour

With the help of the steady shear rheological experiments, the magnetorheological behaviour of the both suspensions based on bare CI particles and suspensions based on ZnO/CI core-shell urchin-like ones in the absence as well as in the presence of the various magnetic flux densities was investigated. As can be seen in the Figure 7 both samples exhibit nearly Newtonian behaviour in the absence of the external field. However, after application of the external field the shear stresses increase with increasing magnetic flux density (Figure 7a) for suspension based on bare CI particles. Values of the yield stress represented by the presence

of the internal structures are not as high as would be expected for the material with such large magnetization saturation. This behaviour is probably connected with the very poor sedimentation stability of the suspension, as was discussed in the previous chapter and particles are not able to develop internal structures with appropriate toughness even at high magnetic flux densities. On the other hand, ZnO/CI core-shell urchin-like particles based suspensions, exhibit higher values of the yield stress than that of bare ones, even the magnetization saturation of ZnO/CI core-shell particles was considerably lower because of presence of coating layer. This behaviour is connected to enhanced sedimentation stability and suspension containing only 20 wt. % particles reaches the value of the yield stress around 0.5 kPa at 272 mT.

Therefore the further investigation was concentrated only on the core-shell particles based suspensions. Figure 8 represents the behaviour of the suspensions of different particle weight fractions (20, 40 and 60) under various magnetic flux densities. Yield stress of all suspensions increases with increasing magnetic flux density and also with particle weight fraction. To properly investigate the impact of the particle concentration on the development of the internal structures the data of the yield stress were fit with power-law relation $\tau_y \approx B^a$ and values of the slope are summarized in the Table 1. As was observed and is usually stated in the literature [34, 43, 44] at low magnetic flux densities the behaviour of suspensions follow dipole mechanism where yield stress, τ_y varies rather with B^2 while at the high magnetic flux densities behaviour of suspensions exhibit local magnetization saturation of the particles and development of the internal structures follows saturation mechanism, where τ_y further varies only with $B^{1.5}$. In this case vectors of the magnetization are saturated and ability of the suspensions to develop considerable tougher internal structures with increased magnetic flux densities is not that high as is at lower flux densities. Finally, it can be concluded that suspension consisted of 60 wt. % of ZnO/CI core-shell particles reaches the values of the yield stress nearly around 2.2 kPa at 272 mT. Moreover, critical magnetic flux density (B_c), is shifted towards higher values of B and suspensions with higher particle concentration need higher magnetic flux density to became magnetically saturated Such values are very promising for the utilizing of these suspensions in the real-life applications.

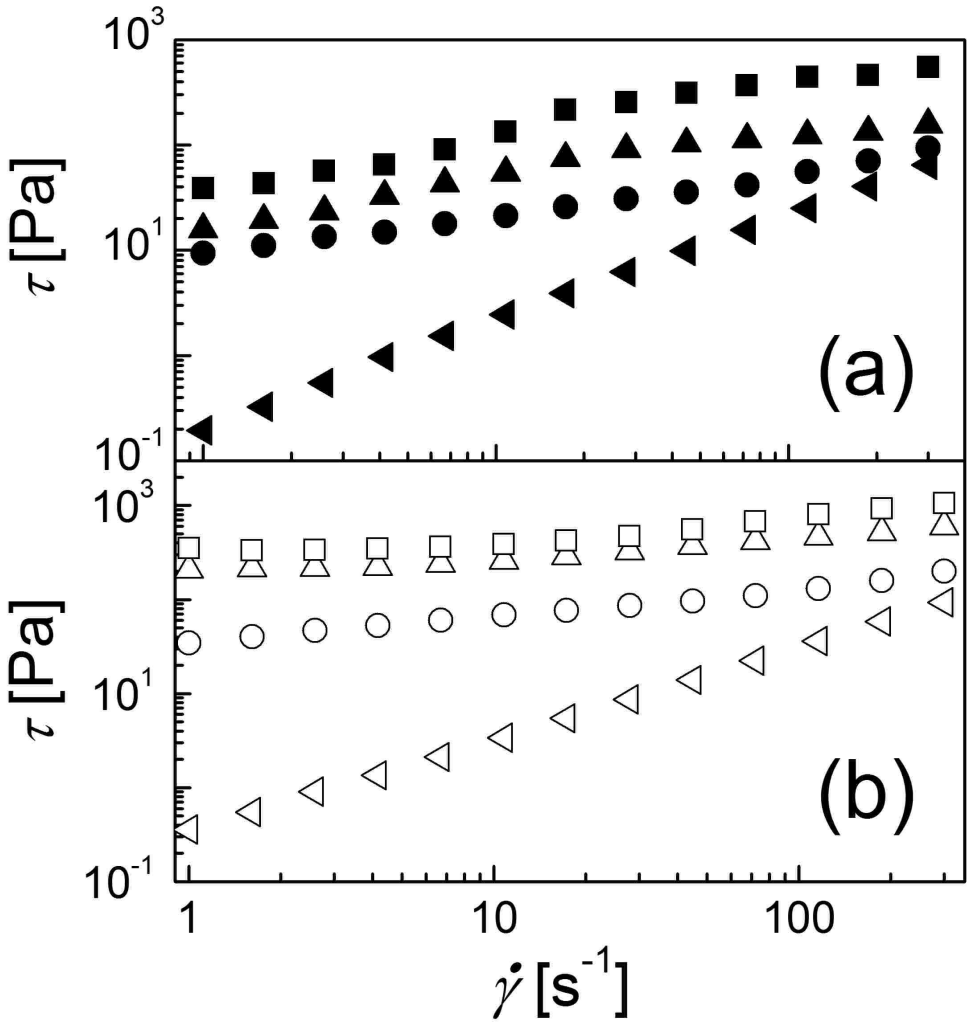

Figure 7: Dependence of the shear stress, τ, on the shear rate, g, for suspensions of 20 wt. % of bare CI particles (a) and ZnO/CI urchin-like particles (b) at various magnetic flux densities, B (mT): (◁, ◀) 0, (●, ○) 45, (▲, △) 132, (■, □) 272.

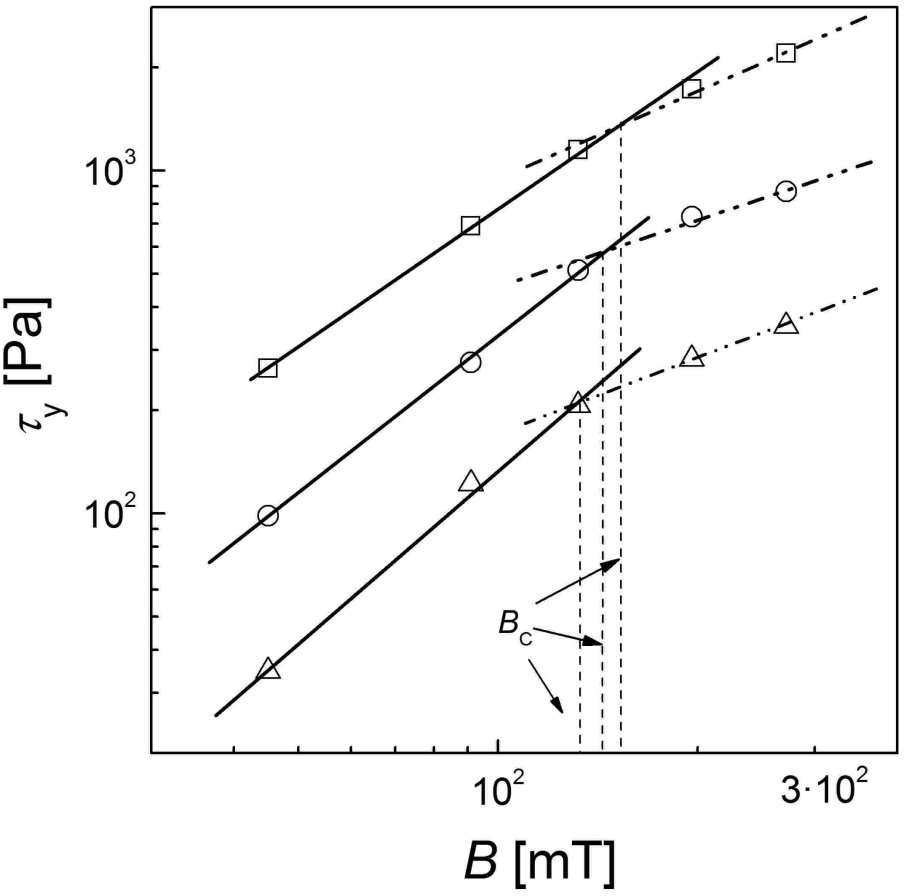

Figure 8: Dependence of the yield stress, τ_y, on the magnetic flux density, B, for suspensions of different particle weight fractions (wt. %): (△) 20, (○) 40, (□) 60. Lines represent the power law model fit of the data for low (solid) and high (dashed) magnetic flux densities.

Table 1: Values of the slope for fitting of data with power-law relation at various magnetic flux densities.

Particle concentration [wt. %]	20	40	60
Low magnetic flux densities	1.90	1.84	1.79
High magnetic flux densities	1.24	1.36	1.52

In applications, the suspensions are usually operating at elevated temperatures. Thus the rheological investigation was performed in the temperature range from 25 to 105°C. For comparison of obtained results MR efficiency $e = (\eta_E - \eta_0)/\eta_0$ rather than absolute values of the yield stresses was selected (Figure 9). The η_E represents the viscosity in the presence of the external magnetic field at low shear rate $g = 1\ s^{-1}$, while η_0 is the viscosity in the absence of the external field at the same shear rate value. There are two reasons of MR efficiency e enhancement at elevated temperatures. In the absence of the external field, viscosity of suspensions η_0 decrease with increasing temperature. In the presence of the external field, magneto-attractive forces between particles are enhanced at elevated temperature and viscosity η_E rises. Therefore, the MR efficiency e increases with increasing temperature and with increasing magnetic flux density.

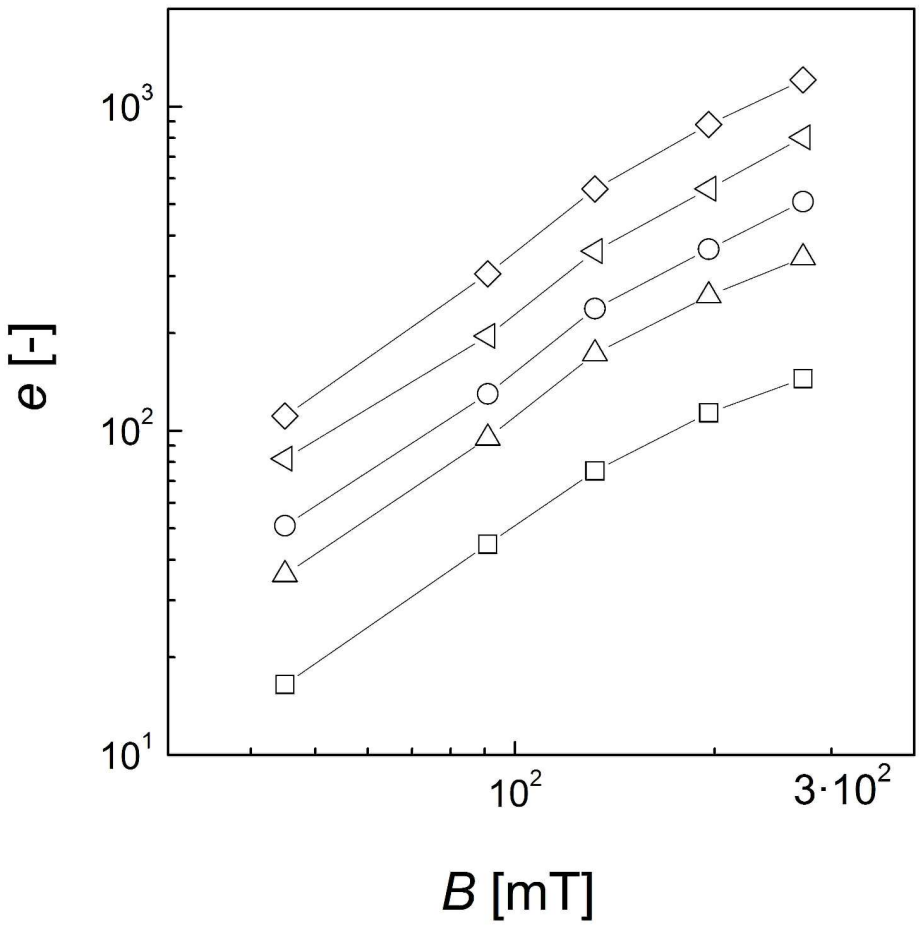

Figure 9: Dependence of the MR efficiency, *e*, on the magnetic flux density, *B*, for suspensions of 60 wt.% of core-shell ZnO/CI particles, at various temperatures *T* (°C): (□) 25, (△) 45, (○) 65, (◁) 85, (◇) 105.

In order to prepare suspensions with improved MR behaviour the bare carbonyl iron particles were mixed with core-shell ZnO/CI urchin-like particles in the ratio 1:1 and silicone oil and the suspension with 20 wt. % of dimorphic particles was obtained. As can be seen in the Figure 10, in the absence of the external electric field strength all suspensions exhibit nearly Newtonian behaviour, the lowest value of viscosity was obtained for bare CI particle-based suspension. Core-shell ZnO/CI particle-based suspensions exhibit higher values of the shear stress due to the ZnO coating of CI which results in enhanced mechanical gripping between particles. In the case of dimorphic particle-based suspension, the dimorphic suspension

character, when bare carbonyl iron particles can fill free space between the core-shell ZnO/CI particles, contributing to the enhanced field-off values of the shear stress. Furthermore, after application of the external magnetic field, the suspension including dimorphic based particles exhibits the highest yield stress in comparison to suspensions consisting of both individual components. This behaviour is probably caused due to the synergism effect coming from the good magnetic properties of bare carbonyl iron and mechanical gripping of core-shell ZnO/CI urchin-like particles.

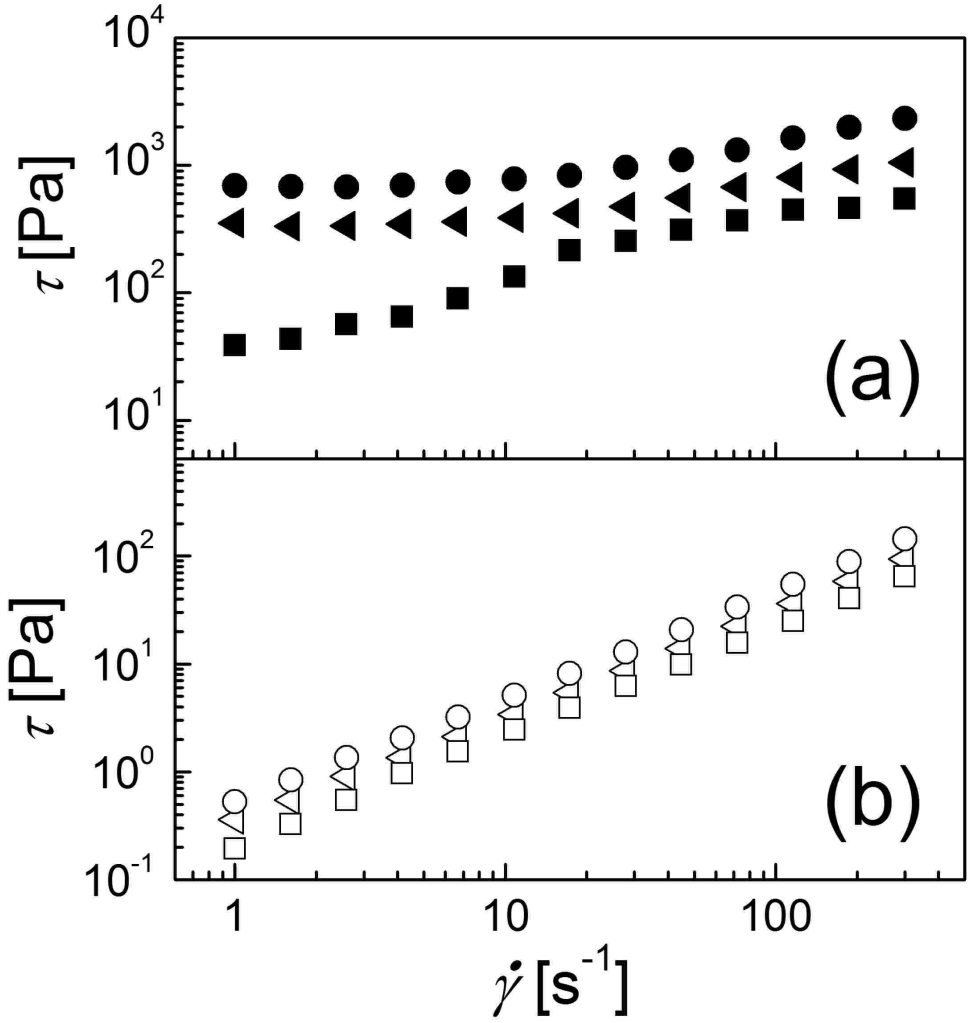

Figure 10: Dependence of the shear stress, τ, on the shear rate, g, for suspensions of 20 wt. % of (■, □) bare CI particles, (◁, ◀) ZnO/CI urchin-like particles and (●, ○) dimorphic particles at 0 mT (b) and (a) 272 mT.

4. Conclusion

A novel two-step synthesis of the core-shell ZnO/CI urchin-like particles was presented. The magnetic properties were shielded by small amount on the ZnO coating on the surface of the CI particles. Furthermore, the thermo-oxidation as well as sedimentation stability were enhanced in case of core-shell based silicone oil suspensions. The rheological investigation also confirmed that core-shell particles based suspensions were able to develop considerable tougher internal structures at 20 wt. % particles concentration than that of bare CI based ones. With increasing core-shell particle concentration in suspension, the yield stress increases and reached values around 2.2 kPa at 272 mT. Furthermore, the critical magnetic flux density (B_c) increases with increasing particle concentration therefore particles need higher B to be magnetically saturated. Finally the suspension based on dimorphic particles was prepared and due to the good magnetization saturation of bare carbonyl iron particles and mechanical gripping of the core-shell ZnO/CI urchin-like particles provides system with highest yield stress in comparison to the both individual components.

Acknowledgement

The authors wish to thank the Grant Agency of the Czech Republic for the financial support of Grant no. 202/09/1626.

This article was written with the support of the Operational Programme 'Education for Competitiveness' co-funded by the European Social Fund (ESF) and the national budget of the Czech Republic, within the project 'Advanced Theoretical and Experimental Studies of Polymer Systems' (reg. number: CZ.1.07/2.3.00/20.0104).

This article was written with the support of Operational Programme 'Research and Development for Innovations' co-funded by the European Regional Development Fund (ERDF) and the national budget of the Czech Republic, within the 'Centre of Polymer Systems' project (reg. number: CZ.1.05/2.1.00/03.0111).

References

[1] G. Bossis; S. Lacis; A. Meunier; O. Volkova, Magnetorheological fluids, J. Magn. Magn. Mater. 252 (2002) 224.

[2] J. D. Carlson; M. R. Jolly, MR fluid, foam and elastomer devices, Mechatronics 10 (2000) 555.

[3] D. J. Klingenberg, Magnetorheology: Applications and challenges, Aiche J. 47 (2001) 246.

[4] B. J. Park; F. F. Fang; H. J. Choi, Magnetorheology: materials and application, Soft Matter 6 (2010) 5246.

[5] J. Pacull; S. Goncalves; A. V. Delgado; J. D. G. Duran; M. L. Jimenez, Effect of polar interactions on the magnetorheology of silica-coated magnetite suspensions in oil media, J. Colloid Interface Sci. 337 (2009) 254.

[6] N. Jain; X. L. Zhang; B. S. Hawkett; G. G. Warr, Stable and Water-Tolerant Ionic Liquid Ferrofluids, ACS Appl. Mater. Interfaces 3 (2011) 662.

[7] Y. D. Liu; F. F. Fang; H. J. Choi, Core-shell-structured silica-coated magnetic carbonyl iron microbead and its magnetorheology with anti-acidic characteristics, Colloid Polym. Sci. 289 (2011) 1295.

[8] M. T. Lopez-Lopez; G. Vertelov; G. Bossis; P. Kuzhir; J. D. G. Duran, New magnetorheological fluids based on magnetic fibers, J. Mater. Chem. 17 (2007) 3839.

[9] C. Magnet; P. Kuzhir; G. Bossis; A. Meunier; L. Suloeva; A. Zubarev, Haloing in bimodal magnetic colloids: The role of field-induced phase separation, Phys. Rev. E 86 (2012) 011404.

[10] K. von Pfeil; M. D. Graham; D. J. Klingenberg; J. F. Morris, Pattern formation in flowing electrorheological fluids, Phys. Rev. Lett. 88 (2002) 188301.

[11] K. von Pfeil; M. D. Graham; D. J. Klingenberg; J. F. Morris, Structure evolution in electrorheological and magnetorheological suspensions from a continuum perspective, J. Appl. Phys. 93 (2003) 5769.

[12] M. T. Lopez-Lopez; P. Kuzhir; G. Bossis; P. Mingalyov, Preparation of well-dispersed magnetorheological fluids and effect of dispersion on their magnetorheological properties, Rheol. Acta 47 (2008) 787.

[13] J. P. Segovia-Gutierrez; C. L. A. Berli; J. de Vicente, Nonlinear viscoelasticity and two-step yielding in magnetorheology: A colloidal gel approach to understand the effect of particle concentration, J. Rheol. 56 (2012) 1429.

[14] F. Vereda; J. de Vicente; J. P. Segovia-Gutierrez; R. Hidalgo-Alvarez, Average particle magnetization as an experimental scaling parameter for the yield stress of dilute magnetorheological fluids, J. Phys. D-Appl. Phys. 44 (2011) 425002.

[15] M. Sedlacik; V. Pavlinek; P. Saha; P. Svrcinova; P. Filip, The Role of Particles Annealing Temperature on Magnetorheological Effect, Mod. Phys. Lett. B 26 (2012) 1150013.

[16] D. Case; B. Taheri; E. Richer, Design and Characterization of a Small-Scale Magnetorheological Damper for Tremor Suppression, IEEE-ASME Trans. Mechatron. 18 (2013) 96.

[17] B. Gonenc; H. Gurocak, Virtual needle insertion with haptic feedback using a hybrid actuator with DC servomotor and MR-brake with Hall-effect sensor, Mechatronics 22 (2012) 1161.

[18] D. M. Wang; Y. F. Hou; Z. Z. Tian, A novel high-torque magnetorheological brake with a water cooling method for heat dissipation, Smart Mater. Struct. 22 (2013) 025019.

[19] X. C. Zhang; Z. D. Xu, Testing and modeling of a CLEMR damper and its application in structural vibration reduction, Nonlinear Dyn. 70 (2012) 1575.
[20] G. M. Kamath; N. M. Wereley; M. R. Jolly, Characterization of magnetorheological helicopter lag dampers, J. Am. Helicopter Soc. 44 (1999) 234.
[21] R. Stanway, Smart fluids: current and future developments, Mater. Sci. Technol. 20 (2004) 931.
[22] M. Sedlacik; R. Moucka; Z. Kozakova; N. E. Kazantseva; V. Pavlinek; I. Kuritka; O. Kaman; P. Peer, Correlation of structural and magnetic properties of Fe3O4 nanoparticles with their calorimetric and magnetorheological performance, J. Magn. Magn. Mater. 326 (2013) 7.
[23] X. Z. Zhang; W. H. Li; X. L. Gong, Thixotropy of MR shear-thickening fluids, Smart Mater. Struct. 19 (2010) 125012.
[24] G. R. Iglesias; M. T. Lopez-Lopez; J. D. G. Duran; F. Gonzalez-Caballero; A. V. Delgado, Dynamic characterization of extremely bidisperse magnetorheological fluids, J. Colloid Interface Sci. 377 (2012) 153.
[25] M. Sedlacik; V. Pavlinek; R. Vyroubal; P. Peer; P. Filip, A dimorphic magnetorheological fluid with improved oxidation and chemical stability under oscillatory shear, Smart Mater. Struct. 22 (2013) 035011.
[26] M. Mrlik; M. Sedlacik; V. Pavlinek; P. Bazant; P. Saha; P. Peer; P. Filip, Synthesis and magnetorheological characteristics of ribbon-like, polypyrrole-coated carbonyl iron suspensions under oscillatory shear, J. Appl. Polym. Sci. 128 (2013) 2977.
[27] M. Sedlacik; V. Pavlinek; M. Lehocky; A. Mracek; O. Grulich; P. Svrcinova; P. Filip; A. Vesel, Plasma-treated carbonyl iron particles as a dispersed phase in magnetorheological fluids, Colloid Surf. A-Physicochem. Eng. Asp. 387 (2011) 99.
[28] M. Sedlacik; V. Pavlinek; P. Saha; P. Svrcinova; P. Filip; J. Stejskal, Rheological properties of magnetorheological suspensions based on core-shell structured polyaniline-coated carbonyl iron particles, Smart Mater. Struct. 19 (2010) 115008.
[29] J. H. Park; B. D. Chin; O. O. Park, Rheological properties and stabilization of magnetorheological fluids in a water-in-oil emulsion, J. Colloid Interface Sci. 240 (2001) 349.
[30] A. Tiraferri; K. L. Chen; R. Sethi; M. Elimelech, Reduced aggregation and sedimentation of zero-valent iron nanoparticles in the presence of guar gum, J. Colloid Interface Sci. 324 (2008) 71.
[31] J. L. Viota; J. de Vicente; J. D. G. Duran; A. Delgado, Stabilization of magnetorheological suspensions by polyacrylic acid polymers, J. Colloid Interface Sci. 284 (2005) 527.
[32] J. L. Viota; A. V. Delgado; J. L. Arias; J. D. G. Duran, Study of the magnetorheological response of aqueous magnetite suspensions stabilized by acrylic acid polymers, J. Colloid Interface Sci. 324 (2008) 199.
[33] J. L. Viota; F. Gonzalez-Caballero; J. D. G. Duran; A. V. Delgado, Study of the colloidal stability of concentrated bimodal magnetic fluids, J. Colloid Interface Sci. 309 (2007) 135.
[34] F. F. Fang; H. J. Choi; W. S. Choi, Two-layer coating with polymer and carbon nanotube on magnetic carbonyl iron particle and its magnetorheology, Colloid Polym. Sci. 288 (2010) 359.
[35] F. F. Fang; H. J. Choi; Y. Seo, Sequential Coating of Magnetic Carbonyliron Particles with Polystyrene and Multiwalled Carbon Nanotubes and Its Effect on Their Magnetorheology, ACS Appl. Mater. Interfaces 2 (2010) 54.

[36] F. F. Fang; Y. D. Liu; H. J. Choi; Y. Seo, Core-Shell Structured Carbonyl Iron Microspheres Prepared via Dual-Step Functionality Coatings and Their Magnetorheological Response, ACS Appl. Mater. Interfaces 3 (2011) 3487.
[37] H. B. Cheng; J. M. Wang; H. R. Ma; P. Hou; J. G. Guan; Q. J. Mang, Stability and Anti-Oxidization of Aqueous MR Fluids Improved by Modifying Iron Particle Surface with Organic Molecule, Acta Phys.-Chim. Sin. 24 (2008) 1869.
[38] M. A. Abshinova; N. E. Kazantseva; P. Saha; I. Sapurina; J. Kovarova; J. Stejskal, The enhancement of the oxidation resistance of carbonyl iron by polyaniline coating and consequent changes in electromagnetic properties, Polym. Degrad. Stabil. 93 (2008) 1826.
[39] Y. H. Kim; J. E. Lee; S. K. Cho; S. Y. Park; I. B. Jeong; M. G. Jeong; Y. D. Kim; H. J. Choi; S. M. Cho, Ultrathin polydimethylsiloxane-coated carbonyl iron particles and their magnetorheological characteristics, Colloid Polym. Sci. 290 (2012) 1093.
[40] Y. D. Liu; H. J. Choi; S. B. Choi, Controllable fabrication of silica encapsulated soft magnetic microspheres with enhanced oxidation-resistance and their rheology under magnetic field, Colloid Surf. A-Physicochem. Eng. Asp. 403 (2012) 133.
[41] M. Mrlik; M. Ilcikova; V. Pavlinek; J. Mosnacek; P. Peer; P. Filip, Improved thermooxidation and sedimentation stability of covalently-coated carbonyl iron particles with cholesteryl groups and their influence on magnetorheology, J. Colloid Interface Sci. 396 (2013) 146.
[42] L. Spanhel; M. A. Anderson, Semiconductor Clusters in the Sol-Gel Process - Quantized Aggregation, Gelation, and Crystal-Growth in Concentrated Zno Colloids, J. Am. Chem. Soc. 113 (1991) 2836.
[43] J. M. Ginder; L. C. Davis, Shear Stresses in Magnetorheological Fluids - Role of Magnetic Saturation, Appl. Phys. Lett. 65 (1994) 3410.
[44] J. M. Ginder; L. C. Davis; L. D. Elie, Rheology of magnetorheological fluids: Models and measurements, Int. J. Mod. Phys. B 10 (1996) 3293.

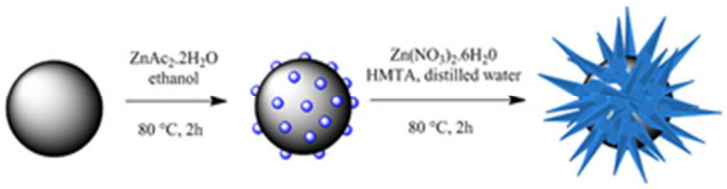

30x7mm (300 x 300 DPI)

Figure captions

Figure 1: XRD patterns of particles, where peaks representing CI are marked as (diamonds) and peaks representing ZnO are marked as (stars).

Figure 2: SEM micrographs of bare CI (a, b), ZnO seeded CI (c, d), ZnO/CI urchin-like (e, f) particles at various magnifications.

Figure 3: EDX spectrum of a surface spot on seeded CI particle, magnified details in inset graph: 1 – C Kα line, 2 – O K Kα line, 3 and 4 – Fe L lines, 5 – Zn L lines, the inset image shows the spot on the CI particle, where the point spectrum was collected from.

Figure 4: VSM spectra of the bare CI (dashed line), ZnO seeded CI (solid line) and ZnO/CI urchin-like (dash dot line) particles.

Figure 5: TGA curves and their derivatives of bare CI (dash dot line) and ZnO/CI urchine-like (solid line) particles.

Figure 6: Sedimentation stability of the bare CI particle suspension measuring jug A (□) and ZnO/CI urchin-like particle suspension measuring jug B (△).

Figure 7: Dependence of the shear stress, τ, on the shear rate, g, for suspensions of 20 wt. % of bare CI particles (a) and ZnO/CI urchin-like particles (b) at various magnetic flux densities, B (mT): (◁, ◀) 0, (●, ○) 45, (▲, △) 132, (■, □) 272.

Figure 8: Dependence of the yield stress, τ_y, on the magnetic flux density, B, for suspensions of different particle weight fractions (wt. %): (△) 20, (○) 40, (□) 60. Lines represent the power law model fit of the data for low (solid) and high (dashed) magnetic flux densities.

Figure 9: Dependence of the MR efficiency, e, on the magnetic flux density, B, for suspensions of 60 wt.% of core-shell ZnO/CI particles, at various temperatures T (°C): (□) 25, (△) 45, (○) 65, (◁) 85, (◇) 105.

Figure 10: Dependence of the shear stress, τ, on the shear rate, g, for suspensions of 20 wt. % of (■, □) bare CI particles, (◁, ◀) ZnO/CI urchin-like particles and (●, ○) dimorphic particles at 0 mT (b) and (a) 272 mT.

Table 1: Values of the slope for fitting of data with power-law relation at various magnetic flux densities.

Particle concentration [wt. %]	20	40	60
Low magnetic flux densities	1.90	1.84	1.79
High magnetic flux densities	1.24	1.36	1.52

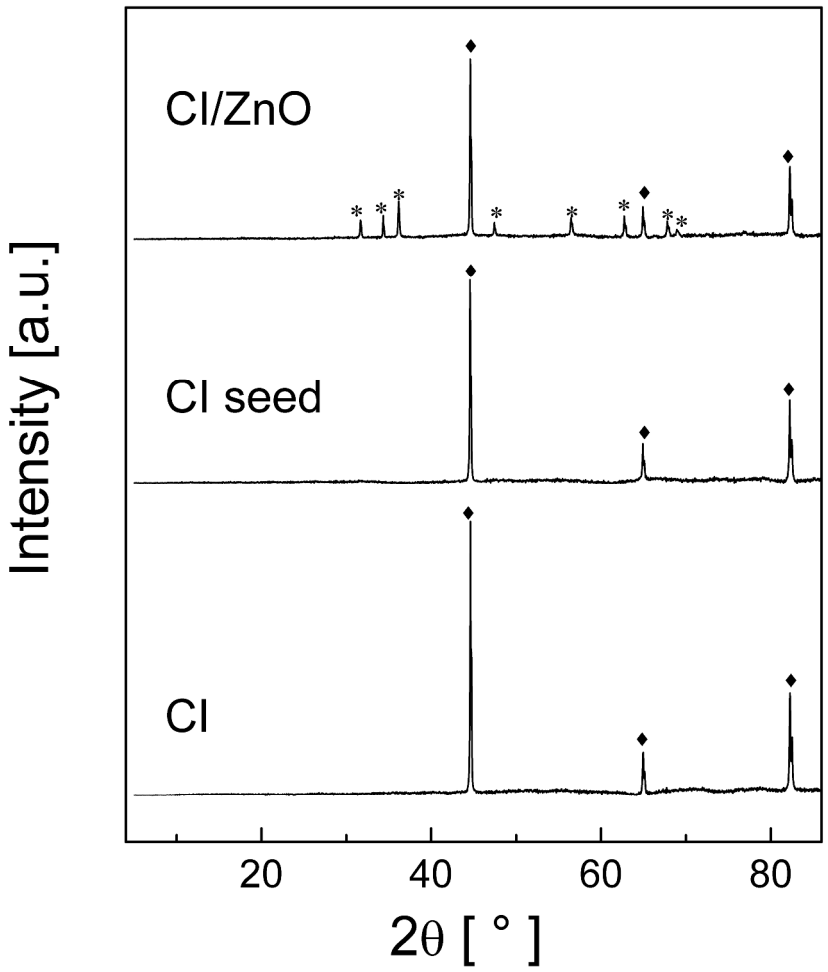

863x894mm (150 x 150 DPI)

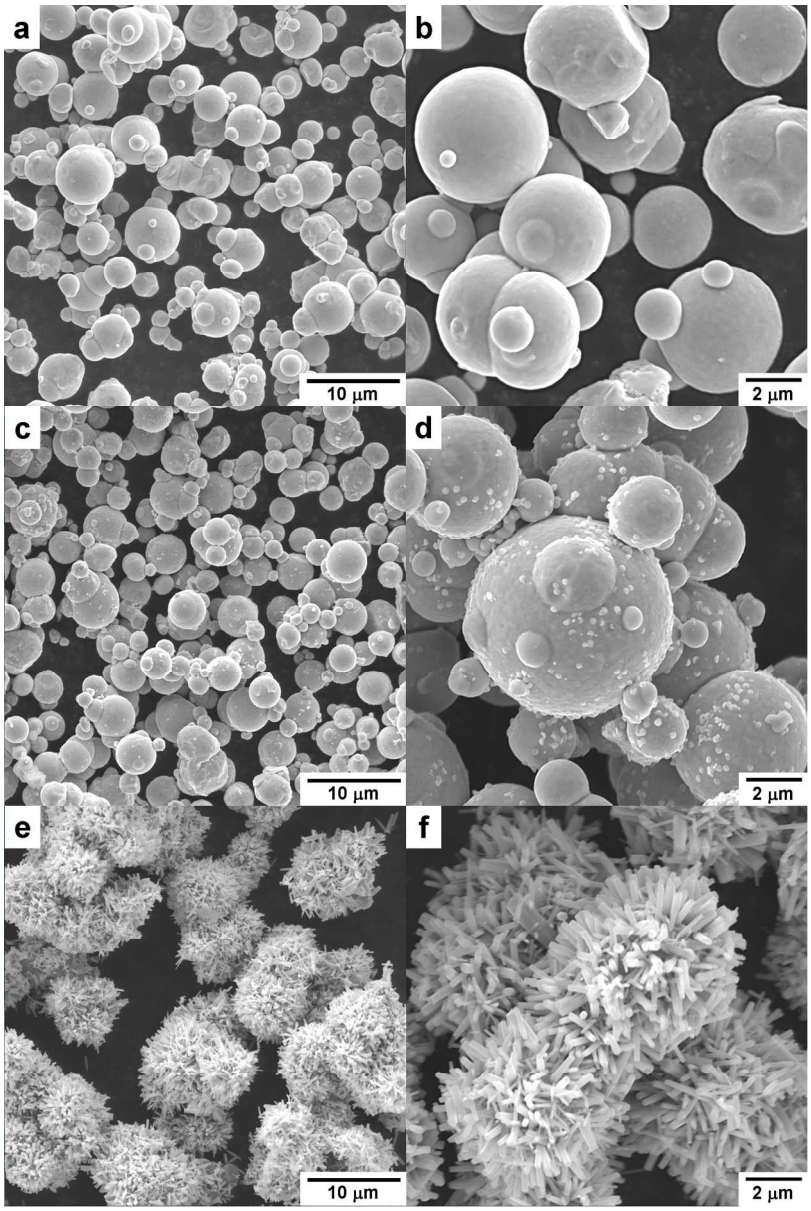

407x609mm (128 x 128 DPI)

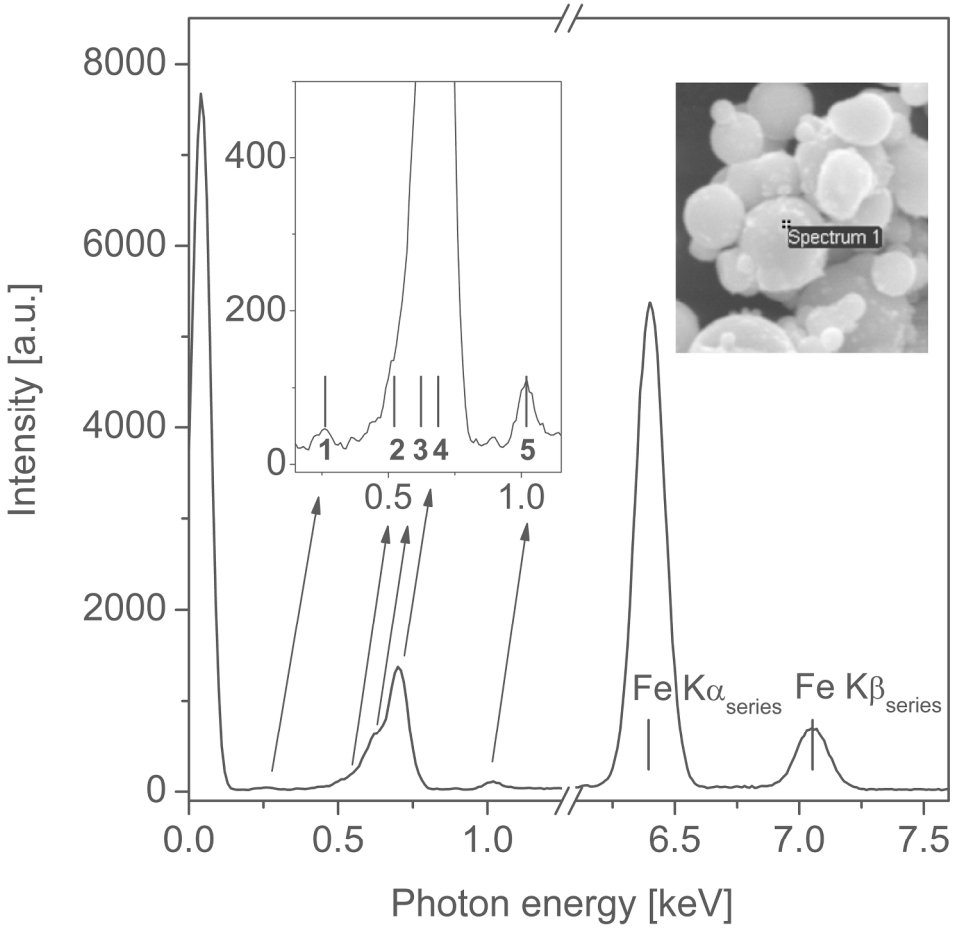

215x208mm (300 x 300 DPI)

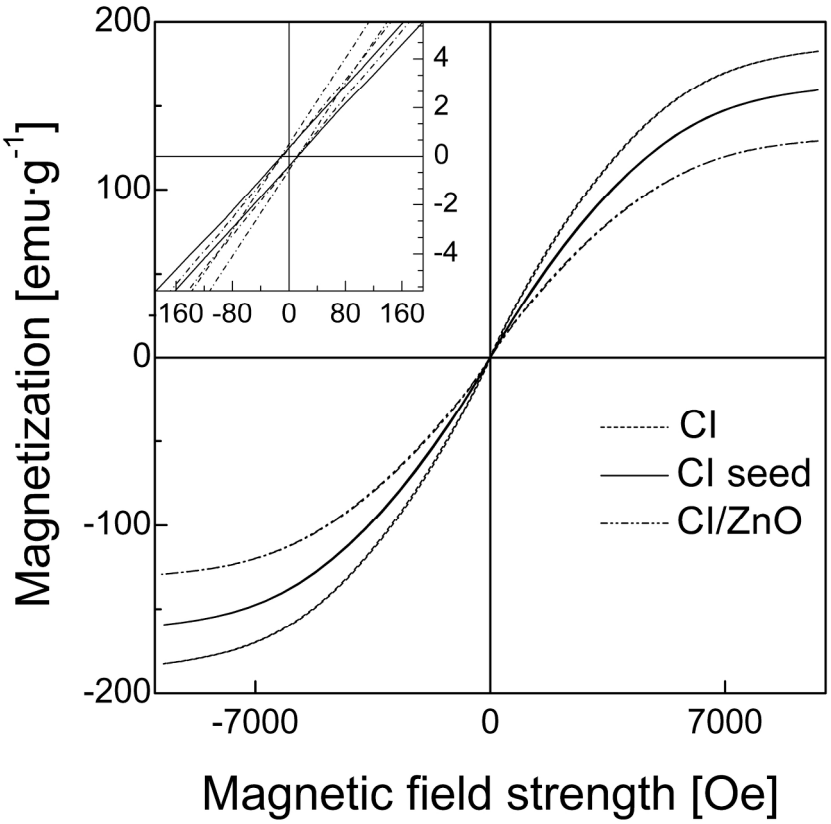

215x208mm (300 x 300 DPI)

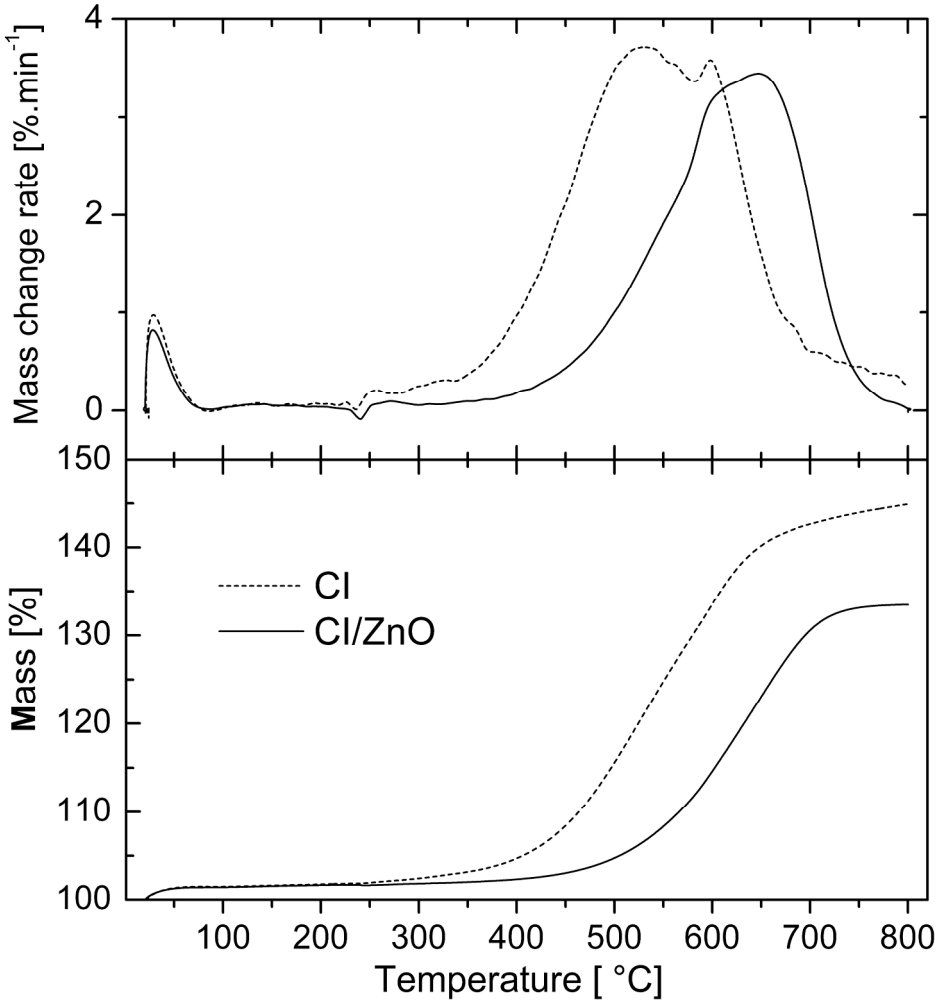

223x231mm (300 x 300 DPI)

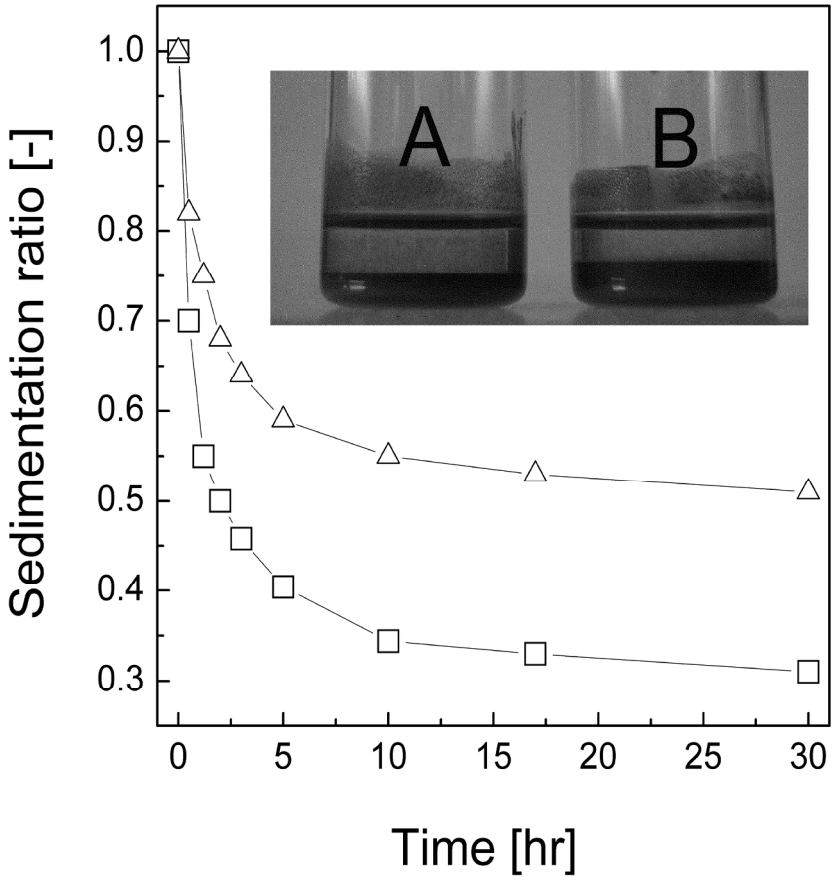

223x231mm (300 x 300 DPI)

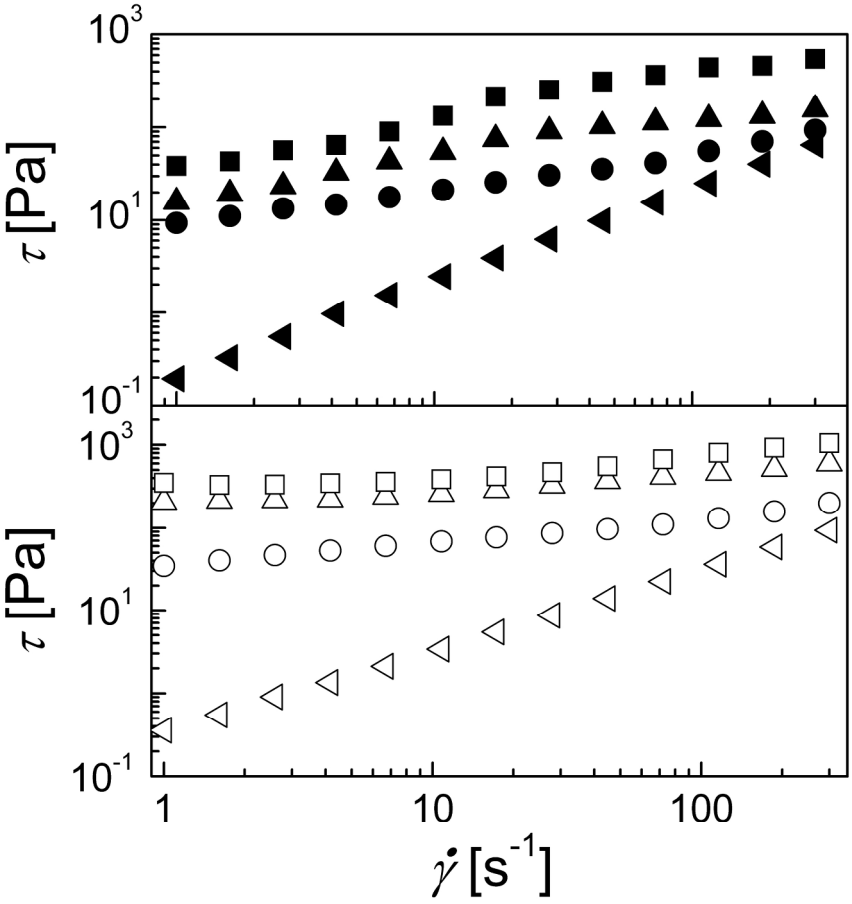

223x231mm (300 x 300 DPI)

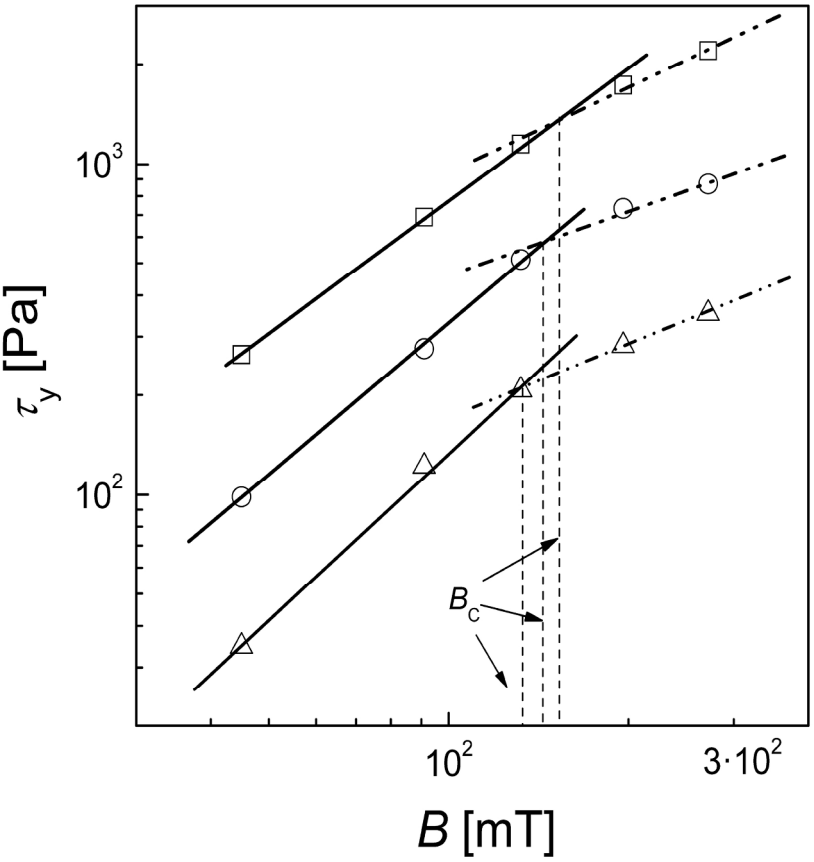

223x231mm (300 x 300 DPI)

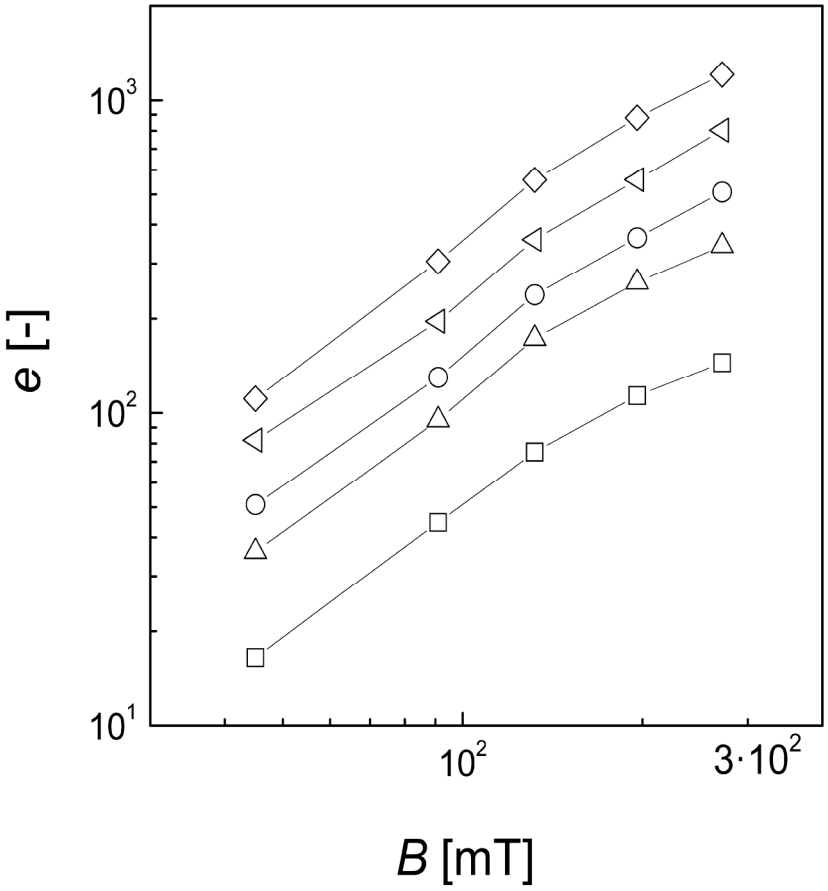

223x231mm (300 x 300 DPI)

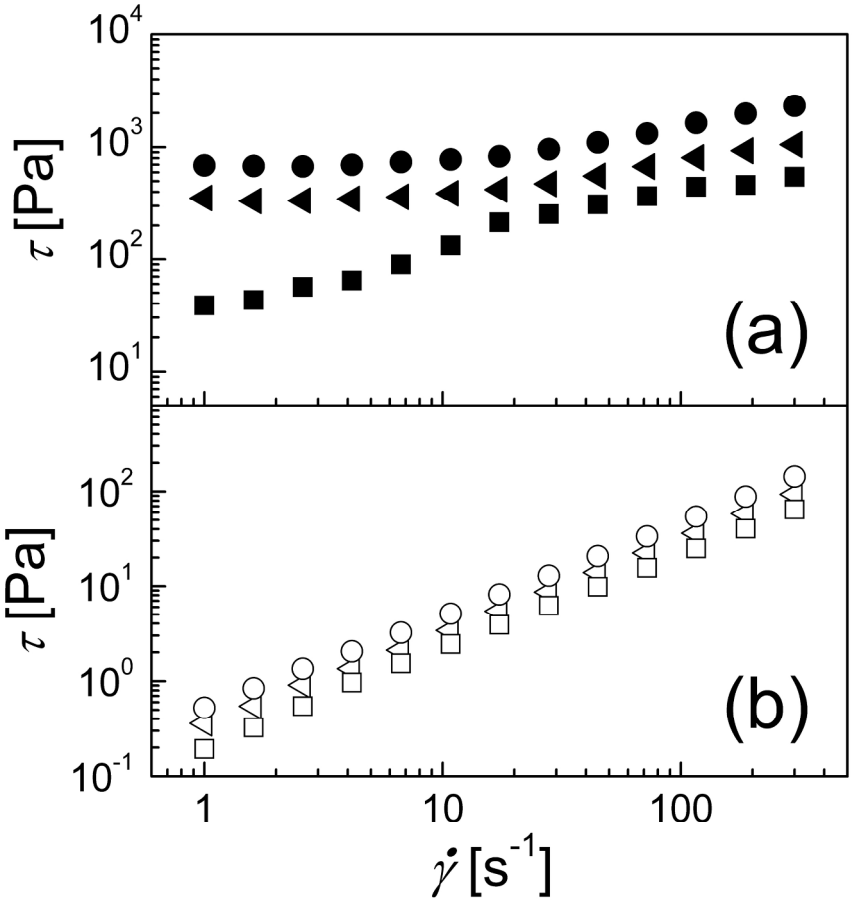

223x231mm (300 x 300 DPI)